



This is an author-deposited version published in: <http://oatao.univ-toulouse.fr/>  
Eprints ID: 4268

**To cite this document:** ILYAS Muhammad, ESPINOSA Christine, LACHAUD Frédéric, MICHEL Laurent, SALAUN Michel. Modelling aeronautical composite laminates behaviour under impact using a saturation damage and delamination continuous material model. *9th International Conference on Fracture and Damage Mechanics*, 20-22 Sept 2010, Nagasaki, Japan.

Any correspondence concerning this service should be sent to the repository administrator: [staff-oatao@inp-toulouse.fr](mailto:staff-oatao@inp-toulouse.fr)

# Modelling Aeronautical Composite Laminates Behaviour under Impact using a Saturation Damage and Delamination Continuous Material Model

Muhammad Ilyas, Christine Espinosa, Frédéric Lachaud, Laurent Michel, Michel Salaün

Institut Clément Ader Université de Toulouse  
Institut supérieur de l'Aéronautique et de l'Espace  
10 Avenue Edouard Belin, 31400 Toulouse

[muhammad.ilyas@isae.fr](mailto:muhammad.ilyas@isae.fr), [christine.espinosa@isae.fr](mailto:christine.espinosa@isae.fr), [frederic.lachaud@isae.fr](mailto:frederic.lachaud@isae.fr),  
[laurent.michel@isae.fr](mailto:laurent.michel@isae.fr), [michel.salaun@isae.fr](mailto:michel.salaun@isae.fr)

**Keywords:** unidirectional composite, damage mechanics, impact, strain rate behavior, numerical simulations.

**Abstract.** We show that the behavior of T700/M21s and T800/M21s composite panels are affected by the influence of strain rates together with local shear and crush punch or global flexural strengths of the structure. A deterministic continuous composite material model has been developed as a LS-DYNA user defined material model for unidirectional composites on the basis of the Matzenmiller model widely used for woven composites. Initiation and evolution up to saturation and fracture are implemented for various and coupled damage mechanisms including delamination. Quasi-static and dynamic characterization tests laminates have been carried out on balanced angle ply  $[\pm\theta]$  and used for calibration of numerical values. Impact induced damage from experiment's measures and numerical predictions are compared for T800/M21S aeronautical samples impacted at 15J.

## Introduction

Where usual rules and design admissible criteria are well known for metallic materials in airplane certification procedures, the global residual strength of composites in case of damage is not well known. Catastrophic cases are the ruin of a structure due to uncontrolled propagation of inner damages. In order to better understand what happens during an impact, and to aid the design of composite structures, it is our aim to experimentally investigate the behavior of T700/M21s and T800/M21s composite panels and to propose a behavior model that could be used to predict the amount of damage after impacts for a wide range of energies or velocities. We present here some part of the work we have done on experimental characterization, theoretical behavior modeling and development. To investigate strain rate effects, 2 real experiments are compared to simulations predictions: one at a low mass and medium velocity, one at a medium mass and a low velocity, both experiment giving the same impact energy of about 15J.

## Experimental characterization T700/T800

**Quasi-Static damage saturation.** 150mmx20mm coupons of T700/M21S and T800/M21S  $[\pm 45^\circ]_{2s}$  were fabricated and tested under quasi-static axial length traction at 2 mm/min that is about  $2 \times 10^{-4} \text{ s}^{-1}$  (Fig. 1a). The general linear elastic behavior of the ply is defined up to 1.2% deformation and a related yield stress of 50 MPa for both materials. Following destructive examination of the tested samples, and considering the different dimension of the T700 and the T800 fiber diameters, it is suggested that the curved part of each curve between 50 MPa and 60 MPa is related to a coupling effect between the inner ply tension and the interface behavior. Above 60 MPa, the T800 based lamina is governed by the interface behavior whereas in the T700 lamina, there is still a competition between the inner ply and the interface irreversible behaviors. It is concluded that the inner plies of both materials can not suffer perpendicular matrix damage higher than a saturation value.

**Dynamic damage and rupture.** Dynamic compression tests have been conducted using a Split Hopkinson Pressure Bar test system at ISAE. Bars are stainless steel 2m long, and 20 mm diameter rods. Different angles were tested at different strain rates in order to identify in one hand the effect of rates on the global behavior, and on a second hand, the contribution of the pure to coupled loadings between inner ply fibers and matrix, and between plies interfaces. Square 20mmx20mm samples of  $[\pm\theta]_{3s}$  were tested at angles of  $15^\circ$ ,  $30^\circ$ ,  $45^\circ$  (Fig. 1b),  $60^\circ$ ,  $75^\circ$ .

The dynamic behaviour of  $[\pm 45^\circ]_{3s}$  is a 4 parts stress-strain curve: 1st linear (up to 1.2% strain), 2nd a curved part passing a maximum stress (at about 2% strain), 3rd a rather linear decreasing part with a strain rate dependent slope (from 3% strain), 4th rupture at a failure strain increasing with increasing the strain rate (always  $\leq 10\%$ ). Other angles do not exhibit the third part of the curves. Apparent rigidities are all about 20GPa ( $\pm 2$  GPa depending on strain rate). As for QS testing, using destructive analysis and previous studies observations [5], it is suggested that the 2nd part is the coupling of inner and inter ply irreversible behavior (onset of damage) and the 3rd part is related to interfaces and parallel matrix cracking only present at  $[\pm 45^\circ]$  interfaces. It is suggested that the fourth part of the curves is related to damage saturation in the ply of T800/M21s samples. Since the deformation yield is always the same, whatever the strain rate, it is supposed that the saturation damage is also the same. The growth of damage and the consequent maximum stress level in the 2nd part of the curves are strain rate dependent above a reference level of  $750s^{-1}$ . Strength versus strain rate has been interpolated (Fig. 1c) using Eq. 1.

$$S_{\max} = S_0 \cdot \left( 1 + C \log \left( \frac{\dot{\epsilon}}{\dot{\epsilon}_{ref}} \right) \right) \quad \text{with } c=4,7 \text{ and } S_0=120 \text{ MPa.} \quad (1)$$

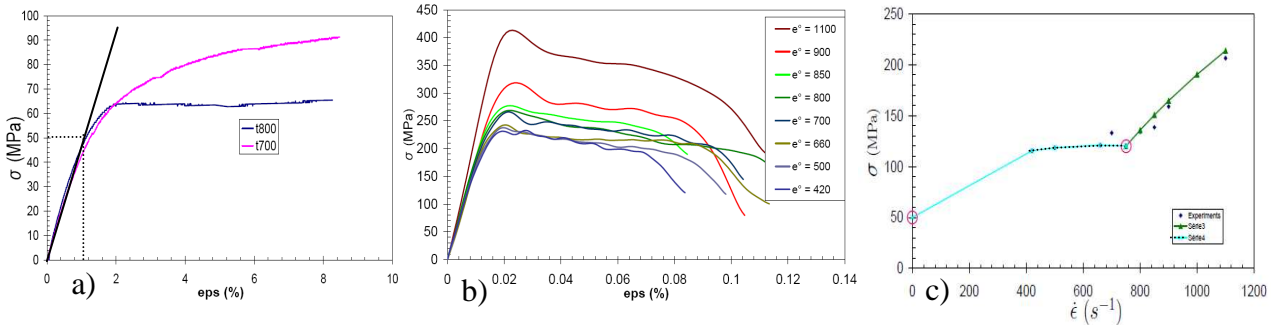


**Figure 1.** a) Quasi-static tension of T700/M21S and T800/M21S  $[\pm 45^\circ]_{2s}$ ; b) Dynamic compression of T800/M21S  $[\pm 45^\circ]_{3s}$ ; c) Strain rate effects on T800/M21S  $[\pm 45^\circ]_{2s}$  lamina strength.

## Material model

**Starting model.** The basis material model is the non linear elastic anisotropic continuum damage mechanics one developed by Matzenmiller &al. [1]. As done “classically”, damage is modeled through its effect on the elastic rigidity loss in further loading or unloading until the damage reaches the value of 1 meaning rupture. The model has been generalized by Xiao &al. [2] for 3D composites and essentially used for woven composites with success for high energy impacts. The model distinguishes 6 damage variables  $\{\omega_i\}$ ,  $i=1,6$  and 5 ruin modes  $\{r_j\}$ ,  $j=1,5$ . The onset and growth of the damage variables can be expressed as a linear combination of the thresholds evolution or using maximum values with the following expressions where  $q_{ij}$  is a coupling tensor between the individual damage modes  $\omega_i$  and the thresholds  $r_j$  and  $m$  is a strain softening parameter that can be adjusted separately for each mode (Eq. 7).

**New criteria for UD.** New failure criteria are proposed hereafter. Note that when  $\omega_2$  reaches saturation then  $\omega_4$  and  $\omega_5$  are saturated too, leading to a failed  $E_{22}$   $G_{12}$  and  $G_{23}$ . The summation method is chosen with a coupling tensor given in Eq. 7.

$$f_1(\sigma, \omega, r) = \left[ \frac{\langle \sigma_{11} \rangle}{X_T} \right]^2 + \left[ \frac{\sigma_{12}^2 + \sigma_{13}^2}{S_{fs}^2} \right] - r_1^2 = 0 \quad \text{Tension/Shear.} \quad (2)$$

$$f_2(\sigma, \omega, r) = \left[ \frac{\langle -2\sigma_{11} + \langle -\sigma_{22} - \sigma_{33} \rangle \rangle}{2X_C} \right]^2 - r_2^2 = 0 \quad \text{Compression.} \quad (3)$$

$$f_3(\sigma, \omega, r) = \left[ \frac{\langle -\sigma_{11} - \sigma_{22} - \sigma_{33} \rangle}{3Z_C} \right]^2 - r_3^2 = 0 \quad \text{Crush.} \quad (4)$$

$$f_4(\sigma, \omega, r) = \left[ \frac{\langle \sigma_{22} \rangle}{X_C} \right]^2 + \left[ \frac{\langle -\sigma_{22} \rangle}{Y_C} \right]^2 + \left[ \frac{\sigma_{12}}{S_{12} + \langle -\sigma_{22} \rangle \tan \varphi} \right]^2 + \left[ \frac{\sigma_{23}}{S_{23} + \langle -\sigma_{22} \rangle \tan \varphi} \right]^2 - r_4^2 = 0 \quad \text{Perp. matrix.} \quad (5)$$

$$f_5(\sigma, \omega, r) = \left[ \frac{\langle \sigma_{33} \rangle}{Z_T} \right]^2 + \left[ \frac{\sigma_{13}}{S_{13} + \langle -\sigma_{33} \rangle \tan \varphi} \right]^2 + \left[ \frac{\sigma_{23}}{S_{23} + \langle -\sigma_{33} \rangle \tan \varphi} \right]^2 - r_5^2 = 0 \quad \text{Parallel matrix.} \quad (6)$$

$$[q] = \begin{bmatrix} 1 & 1 & 1 & 0 & 0 \\ 0 & 0 & 1 & 1 & 0 \\ 0 & 0 & 1 & 0 & 1 \\ 1 & 1 & 1 & 1 & 1 \\ 0 & 0 & 1 & 1 & 1 \\ 1 & 1 & 1 & 0 & 1 \end{bmatrix} \quad \omega_i(\sigma, \omega, \dot{\epsilon}) = \sum_{j=1}^5 q_{ij} \phi_j(\sigma, \omega, \dot{\epsilon}) \quad \phi_j = 1 - e^{\frac{1}{m}(1-r_j^m)}, \quad r_j \geq 1 \quad \text{Coupling.} \quad (7)$$

**Calibration of material properties.** Comparisons between QS and dynamic tests and simulations have been done for T800/M21S determine the following values, and the flexural Young modulus following previous work recommendations [5].

$E_{11} = 165 \text{ GPa}$	$E_{22} = 7.64 \text{ GPa}$	$E_{33} = 7.64 \text{ GPa}$	$E_f = 112 \text{ GPa}$	$X_T = 2.2 \text{ GPa}$	$X_C = 1.2 \text{ GPa}$
$\nu_{21} = 0.016162$	$\nu_{31} = 0.016162$	$\nu_{32} = 0.4$	$m_i = 10$	$Y_T = 45 \text{ MPa}$	$Y_C = 280 \text{ MPa}$
$G_{12} = 5.61 \text{ GPa}$	$G_{23} = 2.75 \text{ GPa}$	$G_{13} = 5.61 \text{ GPa}$	$Z_T = 45 \text{ MPa}$	$Z_C = 0.7 \text{ GPa}$	$S_{ffc} = 0.5 \text{ GPa}$
$S_{12} = 0.05 \text{ GPa}$	$S_{23} = 0.05 \text{ GPa}$	$S_{31} = 0.05 \text{ GPa}$	$S_{fs} = 1.5 \text{ GPa}$	$\omega_{\max} = 0.87$	$\varphi = 10^\circ$

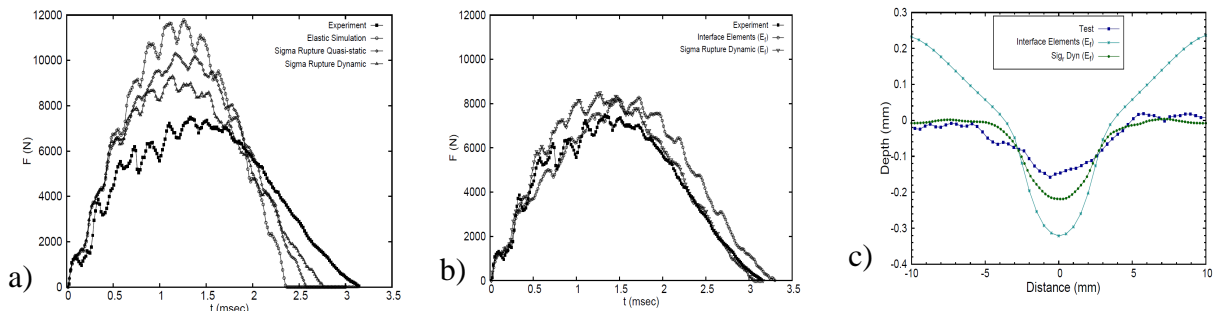
**Table 1.** Data set for our model.

### Application to impact on T800

Impact tests and the corresponding numerical simulations have been performed on simply supported laminates [-45/+45/0/90/0/0/-45/+45/0]s 150mmx100mm T800/M21S panels at about 15J, with two different couples of mass and velocities for the projectile: drop tower (2.368kg, 3,47m/s), canon (17g, 40,82m/s). Results under consideration are the global behavior of the impacted plates given by the force versus time and external craters, and strain rate effects on damage predictions.

**Numerical model.** The numerical model is composed of 8 nodes solid elements, one element per ply in the thickness. The support is rigid as is the projectile and contact are introduced with the plate.

**Global behavior.** Models presented on Fig. 2a are a drop test curve (Test; 7400N/3.17ms) and numerical curves using tensile  $E_{11}$  Young modulus with elastic plies (simu\_elastic), or with our model and a constant quasi static strength of 50 MPa (sigr\_qst), or with our model and the strain rate dependent strength (sigr\_dyn). Fig. 2b shows the drop test curve and numerical curves using the flexural modulus  $E_f$  with a cohesive interface (int\_coh\_flex) previous model [6], or with our model and the strain rate dependent strength (sigr\_dyn\_flex; 8300N/3.05ms). Errors are 12%/4% in force/time.



**Figures 2. a) and b) Force [N] versus time [ms] history curves; c) Indentations [mm].**

On Fig. 2a and 2b, the first linear elastic part is well recovered by all the models (up to 0,7 ms), even though it is obvious that the global rigidity is better retrieved with the flex-modulus. Between

$t=0,7ms$  and  $t= 1,5 ms$ , the global frequency of vibration is correctly recovered with the strain rate dependent models, especially our *dyn\_flex* model even if slightly delayed in time. After a small plateau  $1,5-1,7 ms$  our model and the experimental curve decrease identically down to  $3 ms$ .

Numerical indentation (relative displacement of the upper and bottom faces) at max force time (Fig. 2c) show a promising numerical prediction with our model also compared with a cohesive model we previously developed [6]. Typical values are 0.16 mm for test, 0.22 mm for our *dyn\_flex* model, 0.32 mm for the cohesive model. Note that the indent has been measured 48h after the test while the numerical depth does not take into account any dynamic relaxation.

**Strain rate effects.** The spatial localization of elements failed by saturation in the *dyn\_flex* model (Fig. 3b) gives a prediction of the delaminated area ( $0^\circ\_26,5mm$ ,  $90^\circ\_24mm$ ) similar to what can be observed on C-Scan after a 15J Drop Tower test ( $0^\circ\_25,5mm$ ,  $90^\circ\_29mm$ ). Our previous cohesive model is more diffusive ( $0^\circ\_33,5mm$ ,  $90^\circ\_39mm$ ), as is also the *qst* model.

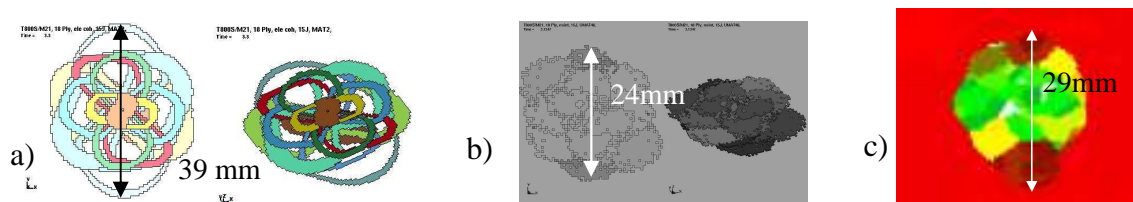


**Figure 3.** a) Delaminated cohesive or b) saturated elements model, and c) DT 15J C-Scan.

## Conclusion

In this study a composite damage material model has been presented that is able to cover a wide range of strain rate loadings, while calibrated up to now with strain rates lower or equal to  $10^3s^{-1}$ . On the experiments analysis, we have proposed and presented our model that consists in proposing new damage criteria and coupling for UD aeronautical composites in the basis model of Matzenmiller & al. and Xiao & al.. A saturation effect was observed for both T700 and T800/M21s samples and taken into account in the dynamic model. The experimentally determined data set has been used to predict impact induced damage with an acceptable ability of the model to represent both the global flexural and vibrating behavior and the local outer indent and inner damages suffered by the composite plates. Further work consist in doing tests at higher strain rates, realizing numerical design simulations to better identify the limitation of our model, improve the cohesive model by adding rate effects, and better use it to establish links between the outer indent and the inner damages at various impact levels.

## Acknowledgement

The authors are grateful of Higher Education Commission of Pakistan for partial funding. Special thanks are also extended to IMPETUS Afea France and all the students and technical staff of ISAE for their valuable input towards numerical and experimental aspects, respectively.

## References

- [1] Matzenmiller A., Lubliner R.L., Taylor A., *A constitutive model for anisotropic damage in fiber composites*, Mechanics of Materials, Vol. 20 (1995), pp 125-152
- [2] Xiao J.R., Gama, B.A., Gillespie J.W. Jr., *Progressive damage and delamination in plain weave S-2 glass/SC-15 composites under quasi-static punch-shear loading*, Composites Structures, Vol. 78 (2007), pp 182-196
- [3] LSTC, LS-DYNA theory manual, ISBN 0-9788540-0-0 (2006)
- [4] Prombut, P., *Caractérisation de la propagation de délaminage des stratifiés composites multidirectionnels*. PhD thesis (2007), Université de Toulouse.
- [5] Ilyas M., Espinosa Ch., Lachaud F., Salaün M., *Dynamic delamination using cohesive finite elements*, DYMAT 2009